May 2002

Contrast mechanism maps for piezoresponse force microscopy

Sergei V. Kalinin
University of Pennsylvania

Dawn A. Bonnell
University of Pennsylvania, bonnell@lrsm.upenn.edu

Copyright Materials Research Society. Reprinted from *Journal of Materials Research*, Volume 17, Number 5, May 2002, pages 936-939.
Publisher URL: http://www.mrs.org/publications/jmr/jmra/articles/2002/may/005.pdf

Contrast mechanism maps for piezoresponse force microscopy

Abstract
Piezoresponse force microscopy (PFM) is one of the most established techniques for the observation and local modification of ferroelectric domain structures on the submicron level. Both electrostatic and electromechanical interactions contribute at the tip-surface junction in a complex manner, which has resulted in multiple controversies in the interpretation of PFM. Here we analyze the influence of experimental conditions such as tip radius of curvature, indentation force, and cantilever stiffness on PFM image contrast. These results are used to construct contrast mechanism maps, which correlate the imaging conditions with the dominant contrast mechanisms. Conditions under which materials properties can be determined quantitatively are elucidated.

Keywords
piezoresponse force microscopy, PFM, ferroelectric domain structures, electromechanical interactions, tip-surface junction, tip radius of curvature

Contrast mechanism maps for piezoresponse force microscopy

Sergei V. Kalinin and Dawn A. Bonnell
Department of Materials Science and Engineering, University of Pennsylvania, 3231 Walnut Street, Philadelphia, Pennsylvania 19104

(Received 20 September 2001; accepted 20 February 2002)

Piezoresponse force microscopy (PFM) is one of the most established techniques for the observation and local modification of ferroelectric domain structures on the submicron level. Both electrostatic and electromechanical interactions contribute at the tip-surface junction in a complex manner, which has resulted in multiple controversies in the interpretation of PFM. Here we analyze the influence of experimental conditions such as tip radius of curvature, indentation force, and cantilever stiffness on PFM image contrast. These results are used to construct contrast mechanism maps, which correlate the imaging conditions with the dominant contrast mechanisms. Conditions under which materials properties can be determined quantitatively are elucidated.

In recent years, piezoresponse force microscopy (PFM)[1] has been successfully employed in the characterization and modification of ferroelectric surfaces on the micron and nanometer level. In PFM, a conductive tip is brought into contact with the surface, and an alternating current (ac) bias, $V_{tip} = V_{dc} + V_{ac}\cos(\omega t)$, is applied to the tip. The piezoelectric response of the underlying surface is detected as the first harmonic component A of the bias-induced tip deflection $d = d_0 + A\cos(\omega t + \varphi)$. The phase φ yields information about the polarization direction below the tip. For domains with polarization vectors pointing downward, the application of a positive tip bias results in the expansion of the sample, and surface oscillations are in phase with the tip voltage, $\varphi = 0$. For domains with polarization vector pointing upward, $\varphi = 180°$. [Often the piezoresponse image is collected as x-Signal $A\cos(\varphi)$.] The piezoresponse amplitude $PR = A/V_{ac}$ defines the local electromechanical activity of the surface and in the early treatments was assumed to be equal or proportional to the piezoelectric constant d_{33} of the material. Numerous observations of local domain dynamics as related to polarization switching, fatigue, phase transitions, etc., have been made.[2–13] Especially of interest are spectroscopic variants of PFM, in which ramping of direct current (dc) voltage offset on the tip V_{dc} allows local hysteresis loops to be acquired.

A determination of local ferroelectric properties, including hysteresis, stress, and size effects, requires quantitative interpretation of the PFM interactions. Both long-range electrostatic forces and the electromechanical response of the surface contribute to the PFM signal so that the experimentally measured piezoresponse is $A = A_{el} + A_{piezo} + A_{nl}$, where A_{el} is electrostatic contribution, A_{piezo} is electromechanical contribution and A_{nl} is nonlocal contribution due to capacitive cantilever–surface interactions.[12] Quantitative PFM imaging requires A_{piezo} to be maximized to achieve predominantly electromechanical contrast.

Contrast in PFM strongly depends on the appropriate choice of the probe, particularly on the cantilever spring constant and tip material. Here we analyze the influence of imaging conditions on the PFM contrast. The magnitudes of A_{el} and A_{piezo} are determined as a function of indentation force and tip radius of curvature. The electrostatic contribution A_{el} is calculated assuming that the total force acting on the tip is composed of the elastic contribution due to the cantilever, $F_0 = kd$, and a capacitive force, $F_{el} = C'(V_{tip} - V_{surf})$,[2] where k is the cantilever spring constant, d is the setpoint deflection, C is the tip-surface capacitance, and V is the potential. The electrostatic interaction is calculated using sphere-anisotropic dielectric plane model and does not depend on the piezoelectric properties of material. The response amplitude is calculated using Hertzian indentation mechanics. For large indentation forces, $F_0 \gg F_{el}$, the linear approximation is valid, $A_{el} \sim (V_{tip} - V_{surf})V_{ac}$. For a typical ferroelectric material with Young's modulus $E^* = 100$ GPa, the electrostatic response is $A_{el} \approx 40$ $(V_{tip} - V_{surf})V_{ac}$ pm. However, the typical potential difference between ferroelectric domains in ambience is small (approximately 150 mV for $BaTiO_3$) due to the polarization screening; therefore, estimated PFM contrast between the domains of opposite polarities is $PR = 6.02$ pm/V. A nonlocal contribution to PFM A_{nl} arises due to the buckling oscillations of the cantilever[14]

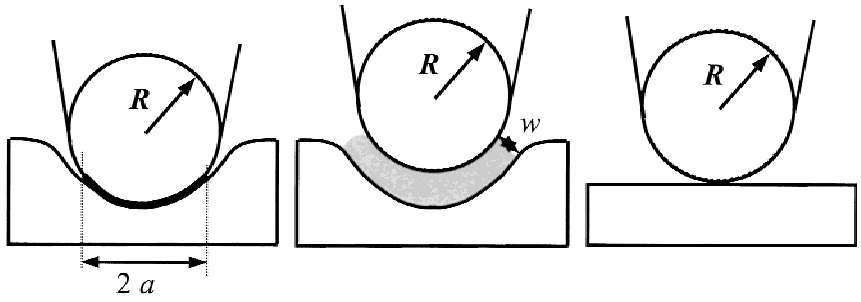

FIG. 1. Limiting cases for the electromechanical interactions in the PFM.

induced by capacitive cantilever–surface interactions.[15] The effective displacement due to the cantilever buckling is inversely proportional to the spring constant of the cantilever, and this effect dominates for cantilevers with relatively small spring constant ($k < 1$ N/m). Typically the cantilever length is significantly larger than the characteristic size of ferroelectric domains; therefore, the nonlocal interaction results in a constant background that does not preclude quantitative domain imaging but heavily contributes to local hysteresis measurements.

In the pure electromechanical case, A_{piezo} depends on the complete set of electroelastic constants of material, as well as tip geometry.[16] Therefore, a relationship between A_{piezo} and materials properties is required. For perfect tip–surface contact $V_{surf} = V_{tip}$ in the contact area, and the electromechanical response of the surface is calculated using the solution for piezoelectric indentation problem by Giannakopoulos and Suresh, [Fig. 1(a)].[17] In this classical, or strong indentation (SI) limit, piezoresponse becomes independent of tip geometry and can be calculated analytically in terms of materials properties. However, the SI limit does not apply to all situations. For example, the high dielectric constant of a ferroelectric material can result in a significant potential drop between the tip and the surface. The effect can be accounted for by introducing a dielectric tip–surface gap that results in the attenuation of tip potential, $V_{surf} = \gamma V_{tip}$ in the contact area, where $\gamma \leqslant 1$ is the attenuation factor determined by gap properties [Fig. 1(b)]. The corresponding regime is referred to as contact limited strong indentation (CSI). The attenuation factor can be estimated as $\gamma = (1 + w\kappa_{eff}/a\kappa_d)^{-1}$, where contact radius a is given by the Hertzian model. Piezoelectric deformation is expected even when the tip is not in contact due to the tip-induced surface charge density. In this case, contact area is negligibly small and $V_{surf} \ll V_{tip}$ [Fig. 1(c)]. This limiting case is referred to as weak indentation (WI). In the WI limit, surface deformation can be calculated using the Greens function for point charge on piezoelectric surface obtained by Karapetian *et al.*[18]

The goal of PFM is to determine the conditions under which quantitative determination of local ferroelectric properties is possible. The tip contribution to the contrast is minimal in the SI limit, and piezoresponse for a variety of ferroelectric materials calculated using published values of electroelastic constants[19,20] is shown in Fig. 2. An almost linear correlation exists between the response in strong indentation limit and d_{33}, $PR \sim 1.5\, d_{33}$. Therefore, despite the significant difference between the boundary conditions in the ideal case (uniform field) and realistic tip–surface geometry, d_{33} provides the dominant contribution to the *PR*. We also find that d_{33} can be determined in the weak indentation limit provided that tip geometry and dielectric properties of material are known.[16] If "true" PFM is the ability to quantify piezoelectric coefficients from the measurements, it can be achieved directly only in the strong indentation region. In the weak indentation regime, the properties of the surface can still

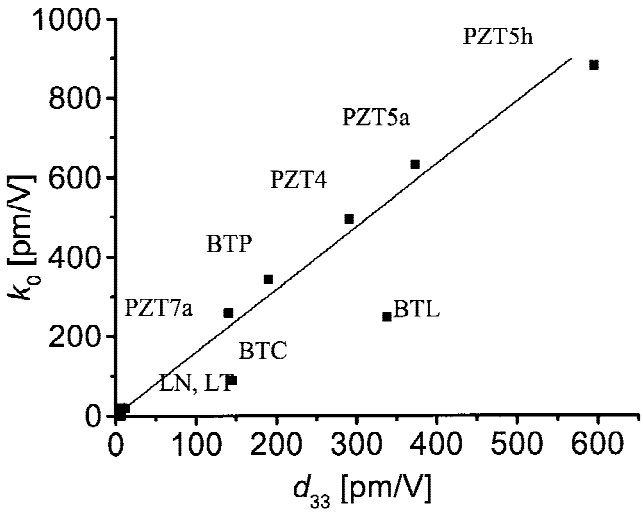

FIG. 2. Correlation between piezoresponse calculated in SI limit and d_{33} for some polycrystal and single crystal materials. PZT denotes different types of commercial lead zirconate-titanate ceramics. LN and LT are $LiNbO_3$ and $LiTiO_3$; BTC is $95\%BaTiO_3/5\%CaTiO_3$ (ceramic B), BTP and BTL are $BaTiO_3$ polycrystals.

be obtained indirectly. Finally, in the electrostatic regime the PFM contrasts by long-range electrostatic interactions, and piezoelectric properties of material are inaccessible.

The variety of tip–surface local and nonlocal interactions necessitates guidelines for quantitative PFM analysis. To relate PFM imaging mechanisms to experimental conditions (tip radius, indentation force, contact area), contrast mechanism maps (CMM) were constructed, as shown in Fig. 3. In the electromechanical case, the effective piezoresponse in the strong indentation limit was taken as 50 pm/V. The boundary between the SI and CSI regimes is calculated with the attenuation factor of 0.3 and the dielectric constant ratio of $\kappa_{eff}/\kappa_d = 30$. The CMM in Fig. 3(a) corresponds to imaging under good tip–surface contact ($w = 0.1$ nm). Less-perfect contact ($w = 1$ nm), which results from oxidized tips or poorly conductive coating, as well as the presence of contaminants, will expand the CSI and nonlinear electrostatic (NE) regions, primarily at the expense of the SI region [Fig. 3(b)]. It should be noted that in the PFM experiment, the wear of the tip results in an increase of contact radius a, to values larger than those predicted by Hertzian mechanics.

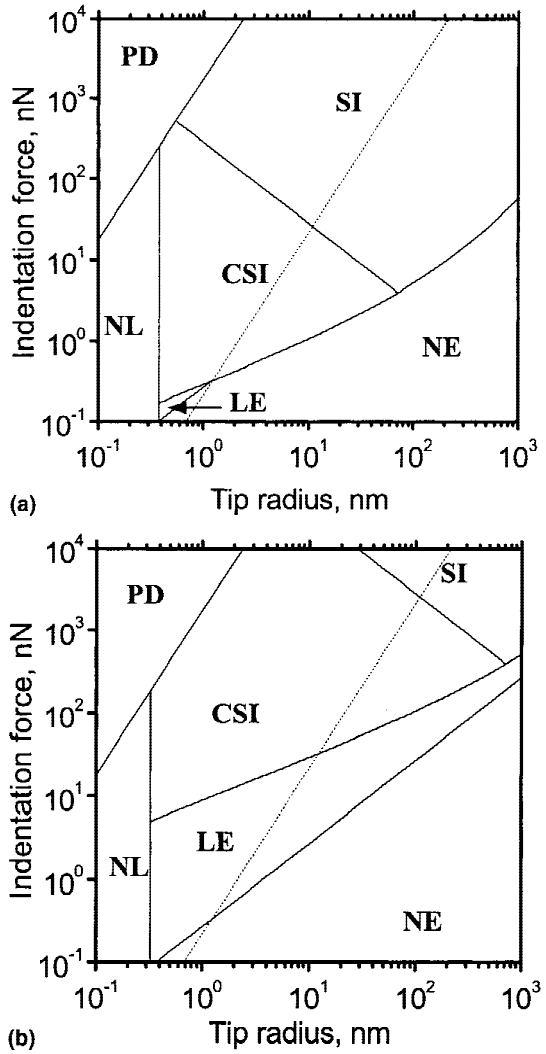

FIG. 3. Contrast mechanism maps of piezoresponse force microscopy. SI is strong indentation regime, WI is weak indentation regime (contact effect), LE is linear electrostatic regime, NE is nonlinear electrostatic regime, NL is non-local interactions due to the PD is plastic deformation. The dotted line delineates the region where stress-induced switching is possible. (a) $w = 0.1$ nm, $\Delta V = V_{tip} - V_s = 1$ V; (b) $w = 1$ nm, $\Delta V = 1$ V.

These results allow multiple controversies in the interpretation of PFM contrast to be reconciled by elucidating experimental conditions under which electrostatic versus electromechanical mechanisms dominate. For example, for a small indentation force, the tip–surface contact area is small and the local electrostatic interactions prevail over the electromechanical response. For larger indentation forces, the tip–surface contact area increases favoring the electromechanical response, while the contact stiffness increases and the electrostatic response decreases. Therefore, the use of relatively stiff cantilevers associated with application of high indentation force

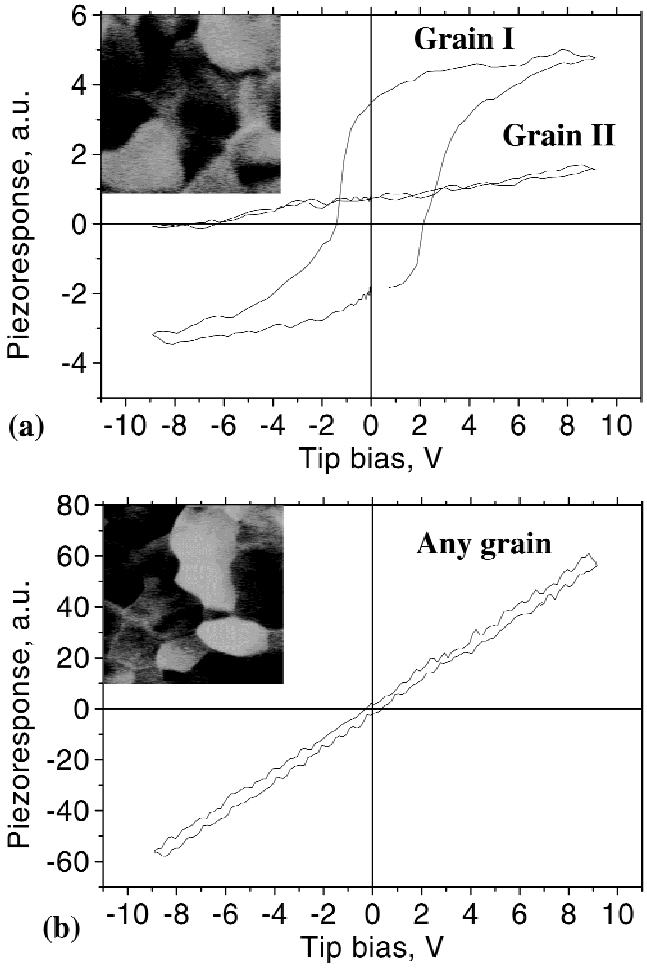

FIG. 4. Piezoresponse hysteresis loops for (a) stiff and (b) soft cantilevers. Upper insets show 1-μm scans of the surface, verifying that imaging is possible in both cases.

favors electromechanical contrast, whereas imaging with soft cantilevers favors electrostatic contrast. It is important to note that polarization suppression below the tip and plastic deformation are possible for very large indentation forces as illustrated in Fig. 3.

The nonlocal cantilever contribution to PFM is illustrated in Fig. 4, which compares local hysteresis loops obtained using cantilevers with large ($k = 5$ N/m) and small ($k = 0.1$ N/m) spring constants. Both cantilevers allow successful PFM imaging since relative domain contrast is not influenced by the nonlocal contribution. However, only the stiff cantilever yields a well-defined local hysteresis loop. The soft cantilever exhibits a response linear in voltage due to the dominance of capacitive cantilever–surface force and cantilever buckling. Nevertheless, the contribution of electrostatic interactions is non-negligible for the first cantilever, as well, and can be detected on nonferroelectric grains (Grain II).

To summarize, to facilitate interpretation of PFM contrast we constructed contrast mechanism maps that correlate the imaging conditions with the image contrast mechanism. These maps are a presentation of analytical solutions associated with various experimental conditions and are compared to experimental measurements. Under some conditions, i.e. those corresponding to relatively large indentation forces and tip radii, the actual piezoelectric coefficient can be determined. This analysis reconciles existing discrepancies in the interpretation of PFM imaging contrast.

ACKNOWLEDGMENTS

The authors acknowledge the financial support from National Science Foundation (NSF) Grant No. DMR 00-79909 and NSF Grant No. DMR 00-80863. The authors are grateful to Dr. Alexei Gruverman, North Carolina State University, for Strontium-Bismuth Tantalate samples.

REFERENCES

1. O. Kolosov, A. Gruverman, J. Hatano, K. Takahashi, and H. Tokumoto, Phys. Rev. Lett. **74,** 4309 (1995).
2. K. Takata, K. Kushida, K. Torii, and H. Miki, Jpn. J. Appl. Phys. **33,** 3193 (1994).
3. C.S. Ganpule, V. Nagarjan, H. Li, A.S. Ogale, D.E. Steinhauer, S. Aggarwal, E. Williams, R. Ramesh, and P. De Wolf, Appl. Phys. Lett. **77,** 292 (2000).
4. A. Gruverman and Y. Ikeda, Jpn. J. Appl. Phys. **37,** L939 (1998).
5. S. Hong, E.L. Colla, E. Kim, K. No, D.V. Taylor, A.K. Tagantsev, P. Muralt, and N. Setter, J. Appl. Phys. **86,** 607 (1999).
6. J.A. Christman, S.H. Kim, H. Maiwa, J.P. Maria, B.J. Rodriguez, A.I. Kingon, and R.J. Nemanich, J. Appl. Phys. **87,** 8031 (2000).
7. S.V. Kalinin and D.A. Bonnell, J. Appl. Phys. **87,** 3950 (2000).
8. E.Z. Luo, Z. Xie, J.B. Xu, I.H. Wilson, and L.H. Zhao, Phys. Rev. B **61,** 203 (2000).
9. V. Likodimos, M. Labardi, and M. Allegrini, Phys. Rev. B **61,** 14440 (2000).
10. J. Munoz-Saldana, G.A. Schneider, and L.M. Eng, Surf. Sci. **480,** L402 (2001).
11. A. Gruverman, O. Auciello, and H. Tokumoto, Annu. Rev. Mater. Sci. **28,** 101 (1998).
12. J.W. Hong, K.H. Noh, S.I. Park, S.I. Kwun, and Z.G. Kim, Rev. Sci. Instrum. **70,** 1735 (1999).
13. L.M. Eng, H-J. Guntherodt, G.A. Schneider, U. Kopke, and J. Munoz Saldana, Appl. Phys. Lett. **74,** 233 (1999).
14. S.V. Kalinin and D.A. Bonnell (unpublished).
15. S. Hong, J. Woo, H. Shin, J.U. Jeon, Y.E. Pak, E.L. Colla, N. Setter, E. Kim, and K. No, J. Appl. Phys. **89,** 1377 (2001).
16. S.V. Kalinin and D.A. Bonnell, Phys. Rev. B Phys. Rev. B **65,** 12408 (2002).
17. A.E. Giannakopoulos and S. Suresh, Acta Mater. **47,** 2153 (1999).
18. E. Karapetian, I. Sevostianov, and M. Kachanov, Philos. Mag. B **80,** 331 (2000).
19. Landolt-Bornstein New Series, edited by K-H. Hellwege and A.M. Hellwege, (Springer-Verlag, New York, 1981), Vol. 16a.
20. D. Berlincourt, in *Ultrasonic Transducer Materials*, edited by O.E. Mattiat (Plenum Press, New York, 1971).